Wave-Induced Momentum Transport and Flow Drive in Tokamak Plasmas

L. A. Berry, E. F. Jaeger, and D. B. Batchelor
Oak Ridge National Laboratory, Oak Ridge, Tennessee 37831-8071
(Received 24 August 1998)

Wave-induced flows are calculated from high-resolution electromagnetic field calculations with either a compressible Reynolds stress or a second-order kinetic pressure model for the radio frequency forces. Results show that electron Landau damping and magnetic pumping, by themselves, do not lead to significant poloidal flow as long as there is little net input of momentum by the wave. But ion-cyclotron damping of either fast magnetosonic waves or ion-Bernstein waves can drive significant poloidal flows at power levels typical of plasma-heating experiments. [S0031-9007(99)08584-1]

PACS numbers: 52.50.Gj, 52.35.Ra, 52.55.Fa

As presently understood, the development of an attractive magnetic fusion power reactor requires operation in an enhanced confinement mode. These modes are thought to result from the stabilization of plasma turbulence by sheared poloidal rotation [1] and are induced by combinations of wall conditioning and plasma-heating techniques. However, they are difficult to control, and the extension to steady state is uncertain. One method for addressing these issues is the use of externally driven radio frequency (rf) waves [2]. A number of calculations [3–5] and some experiments [6,7] have suggested that a modest amount of power in the ion-cyclotron range of frequencies is sufficient to directly drive the needed plasma flow. Among the waves examined, the ion-Bernstein wave (IBW) has been one of the most promising.

In this Letter we present new assessments of rf flow drive based on high-resolution electromagnetic (EM) field calculations, with either a compressible Reynolds stress or a kinetic pressure model for the rf forces. These models address two key assumptions used in previous analyses: (1) The flow response is incompressible, and (2) the rf pressure can be represented by a Reynolds stress [3–5]. IBWs rely on a compressible plasma response to propagate, and we find that compressibility is also needed to provide even a qualitatively correct understanding of the flow response. Even with the inclusion of compressibility, the Reynolds stress estimate for the rf pressure can be significantly different from the kinetic pressure result when finite Larmor radius effects are important. This is perhaps not surprising because the Reynolds stress approximation is usually invoked for turbulent systems, and its *a priori* validity for coherent waves is not clear.

Results here show that ion-cyclotron damping of either fast waves or IBWs can drive significant poloidal flow at power levels typical of plasma-heating experiments. But electron Landau damping (LD) and transit time magnetic pumping (TTMP), by themselves, do not lead to significant poloidal flow.

We first review previous fluid calculations for the rf forces while retaining finite compressibility. Next, to eliminate the Reynolds stress assumption, a kinetic model for the rf force is developed. Wave-induced poloidal flows are then calculated for both fast magnetosonic waves and directly launched IBWs.

Poloidal flows can be estimated by balancing momentum sources (EM forces and rf pressure gradients) against losses. For a species s with distribution function f_s, the momentum moment of the Vlasov equation gives

$$\frac{\partial}{\partial t}(n_s m_s \mathbf{u}_s) + \nabla \cdot \mathbf{P}_s = n_s q_s(\mathbf{E} + \mathbf{u}_s \times \mathbf{B}) - \mu m_s n_s \mathbf{u}_s , \qquad (1)$$

where $n_s = \int f_s \, d^3v$ is the density, $n_s \mathbf{u}_s = \int \mathbf{v} f_s \, d^3v$ is the particle flux, and $\mathbf{P}_s = m_s \int \mathbf{vv} f_s \, d^3v$ is the pressure. The poloidal momentum loss is given by neoclassical viscosity μ [4,5]. The tokamak is modeled as a one-dimensional (1D) slab where x and y are radial and poloidal coordinates, respectively.

In the center of mass frame [$\mathbf{V} = (1/\rho_m^T)\sum_s m_s n_s \mathbf{u}$ with $\rho_m^T = \sum_s n_s m_s$], the pressure tensor can be expressed as the sum of a "thermal" component,

$$\boldsymbol{\pi} = \sum_s m_s \int f_s(\mathbf{v} - \mathbf{V})(\mathbf{v} - \mathbf{V}) \, d^3v , \qquad (2)$$

and a convective component or Reynolds stress tensor, $\rho_m^T \mathbf{VV}$. Then summing over species, Eq. (1) gives

$$\frac{\partial}{\partial t}(\rho_m^T \mathbf{V}) + \nabla \cdot (\rho_m^T \mathbf{VV}) = -\nabla \cdot \boldsymbol{\pi} + \rho_q^T \mathbf{E} + \mathbf{J} \times \mathbf{B} - \mu \rho_m^T \mathbf{V} , \qquad (3)$$

where $\mathbf{J} = \sum_s n_s q_s \mathbf{u}_s$ and $\rho_q^T = \sum_s n_s q_s$.

We now consider a perturbing rf wave with frequency ω and electric and magnetic fields, $\mathbf{E}_1(\mathbf{r}, t)$ and $\mathbf{B}_1(\mathbf{r}, t) \propto \exp[i(\mathbf{k} \cdot \mathbf{r} - \omega t)]$. Equation (3) is linearized in powers of these rf fields, where first-order (rapid time variation) quantities are denoted by subscript "1," and second-order (slow time variation) quantities by subscript "2." The second-order flow velocity can be found by averaging over time and assuming steady state. The result is

$$\mu \rho_m^{(0)} \mathbf{V}_2 = \langle \rho_q^{(1)} \mathbf{E}_1 + \mathbf{J}_1 \times \mathbf{B}_1 \rangle_t - \nabla \cdot (\rho_m^{(0)} \langle \mathbf{V}_1 \mathbf{V}_1 \rangle_t) + \mathbf{J}_2 \times \mathbf{B}_0 - \nabla \cdot \boldsymbol{\pi}_2 , \qquad (4)$$

where $\langle\,\rangle_t$ represents the time average. The first term on the right is the EM force, and the second is the Reynolds stress. The y component of $\mathbf{J}_2 \times \mathbf{B}_0$ sums to zero by ambipolarity. In addition, previous models have assumed $\nabla \cdot \pi_2 = 0$ and incompressible waves ($\nabla \cdot \mathbf{V}_1 = 0$), yielding for the y component of Eq. (4) [3,4]

$$V_{2,y} = \frac{1}{\mu \rho_m^{(0)}} [\langle \rho_q^{(1)} E_{1,y} + (\mathbf{J}_1 \times \mathbf{B}_1)_y \rangle_t - \rho_m^{(0)} \langle (\mathbf{V}_1 \cdot \nabla) V_{1,y} \rangle_t]. \qquad (5)$$

Because $\mathbf{V}_1$ is mass weighted, ion damping will be more effective in driving flow than will electron interactions.

Previous analyses have, in most instances, implicitly assumed incompressibility by omitting a term from the linearized momentum equation. Using the density moment, the usual form for the left side of Eq. (3) is $\rho_m^T[\partial \mathbf{V}/\partial t + (\mathbf{V} \cdot \nabla)\mathbf{V}]$. Even in steady state, the term $\langle \rho_m^{(1)} \partial \mathbf{V}_1/\partial t \rangle_t$ is present and is equal to $\mathbf{V}_1 \nabla \cdot (\rho_m^{(0)} \mathbf{V}_1)$.

To avoid assuming $\nabla \cdot \pi_2 = 0$, a second-order kinetic analysis is necessary in addition to the usual first-order treatment for $\mathbf{V}_1$. Both are found from solutions to the Vlasov equation,

$$\frac{\partial f}{\partial t} + \mathbf{v} \cdot \nabla f + \frac{q}{m} [\mathbf{E}_1 + \mathbf{v} \times (\mathbf{B}_0 + \mathbf{B}_1)] \cdot \nabla_v f = 0. \qquad (6)$$

The distribution function is expanded in powers of the electric field as $f = f_0 + f_1 + f_2$, where f_0 is the equilibrium solution, f_1 is the linear solution $\propto \exp[i(\mathbf{k} \cdot \mathbf{r} - \omega t)]$, and f_2 is the slowly varying (in time), second-order response. We assume that f_0 is an isotropic Maxwellian and we use the well-known solution for $f_1(\mathbf{r}, \mathbf{v}, t)$ [8]. The second-order, time-averaged Vlasov equation can then be written in terms of f_1 as [9]

$$\frac{\partial f_2}{\partial t} + \mathbf{v} \cdot \nabla f_2 + \frac{q}{m} (\mathbf{E}_0 + \mathbf{v} \times \mathbf{B}_0) \cdot \nabla_v f_2 = -\left\langle \frac{q}{m} (\mathbf{E}_1 + \mathbf{v} \times \mathbf{B}_1) \cdot \nabla_v f_1(\mathbf{r}, \mathbf{v}, t) \right\rangle_t. \qquad (7)$$

Second-order electric fields are neglected in Eq. (7) but are not needed for estimates of the rf forces [10]. Equation (7) can be solved for f_2 by integrating along unperturbed orbits. We choose $f_{2|t=0} = 0$ so that

$$f_2(\mathbf{r}, \mathbf{v}, t) = -\int_0^t dt' \times \left\langle \frac{q}{m} \mathbf{F}(\mathbf{r}', \mathbf{v}', t') \cdot \nabla_{v'} f_1(\mathbf{r}', \mathbf{v}', t') \right\rangle_t. \qquad (8)$$

The total force in the poloidal direction is the sum of the EM force,

$$F_{y,s}^{\mathrm{EM}} = \frac{1}{2} \operatorname{Re} \int d^3 v \, q_s [E_{1,y} + (\mathbf{v} \times \mathbf{B}_1)_y]^* f_{1,s}, \qquad (9)$$

and the y component of the kinetic pressure gradient,

$$(\nabla \cdot \mathbf{P}_2)_{y,s} = \left\langle m_s \frac{\partial}{\partial x} \int d^3 v \, v_x v_y f_{2,s} \right\rangle_t, \qquad (10)$$

where the time average is over a cyclotron period to eliminate the arbitrary initial phase assumed at $t = 0$. Combining Eqs. (9) and (10), the total poloidal flow velocity is given by

$$V_{2,y} = \frac{1}{\mu \rho_m^{(0)}} \langle F_y^{\mathrm{EM}} - (\nabla \cdot \mathbf{P}_2)_y \rangle_t, \qquad (11)$$

where $F_y^{\mathrm{EM}} - (\nabla \cdot \mathbf{P}_2)_y$ is summed over species. To describe rf interactions up to third harmonic, Eq. (11) has been expanded to third order in the ion gyroradius/wavelength.

The rf fields needed for the force balance evaluation are calculated from a full-wave numerical solution to Maxwell's equations [11], which resolves the IBW scale length in 1D. A third-order expansion in ion gyroradius/wavelength is also employed in this calculation. Parameters are modeled after the Alcator C-Mod experiment [12]: major radius $R_0 = 0.67$ m, minor radius $a = 0.20$ m, and magnetic field $B_0 = 4.0$ T on axis. The antenna is located just outside the plasma at $R = 0.88$ m and is characterized by a toroidal wave number $k_z = 10\ \mathrm{m}^{-1}$ and a poloidal wave number $k_y = 0\ \mathrm{m}^{-1}$ (i.e., no net input of poloidal momentum by the wave). Plasma profiles are assumed to be parabolic with central density and temperatures: $n_0 = 1.5 \times 10^{20}\ \mathrm{m}^{-3}$, $T_{e,0} = 2.5$ keV, and $T_{i,0} = 1.5$ keV.

Figure 1 shows the poloidal flow velocity for fast waves launched in a helium-3 (He^3) plasma with 10% minority hydrogen (H). The frequency ($f = 50$ MHz) is near the first harmonic of the minority H, and the power absorbed is 1 MW. To suppress mode conversion to IBW near the two ion hybrid resonance, k_z is chosen artificially large. The poloidal flow velocity is calculated from three different models: (a) incompressible fluid [Eq. (5)], (b) compressible fluid [Eq. (5) with $\nabla \cdot (\rho_m^{(0)} \langle \mathbf{V}_1 \mathbf{V}_1 \rangle)$], and (c) a kinetic rf pressure model [Eq. (11)]. The long dashed line shows the contribution of the EM force (the same for all models), and the short dashed line shows the contribution of the Reynolds stress and/or rf pressure. The solid line shows the total flow velocity. The effect of compressibility in Fig. 1(b) is to slightly reduce the contribution of the Reynolds stress. Kinetic effects in Fig. 1(c) give an rf pressure that is about 20%–30% larger than the Reynolds stress from either of the fluid models. While the kinetic modifications to the rf pressure are relatively small, they are sufficient to reverse the net flow relative to both fluid models. This follows from the near cancellation of the EM and rf pressure forces and highlights the sensitivity of the net flow to details of the model for electromagnetic waves. Results similar to those in Fig. 1 have been found for minority ion-cyclotron damping of fast waves at the second harmonic resonance.

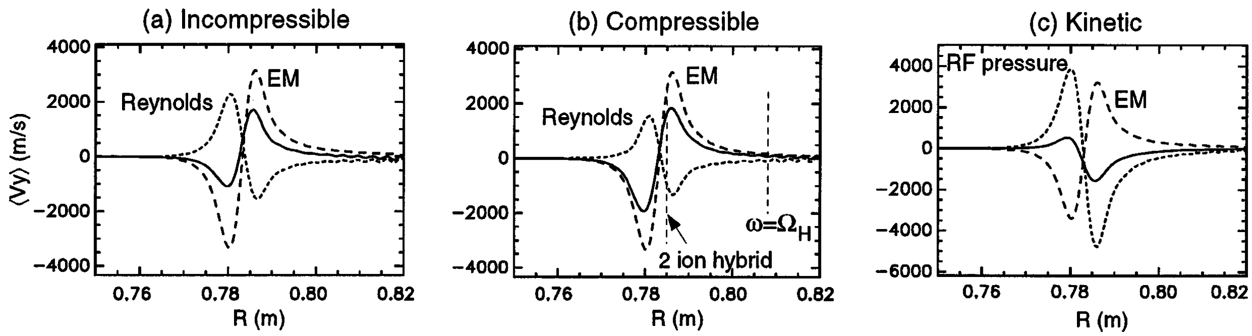

FIG. 1. Poloidal flow velocity for fast waves absorbed near the two ion hybrid resonance with 10% H in He^3, $f = 50$ MHz, $B(0) = 4.0$ T, and $k_z = 26\ \mathrm{m}^{-1}$: (a) incompressible fluid, (b) compressible fluid, and (c) kinetic model.

Figure 2 shows a contrasting result for IBW that is launched directly from the plasma edge. In this case, there are no cyclotron resonances in the region plotted, and all wave damping is due to electron LD and TTMP. The plasma consists of a 2% minority of He^3 in deuterium (D), and the antenna is just in front of the second harmonic of D. Although there is no net input of poloidal momentum ($k_y = 0$), the incompressible fluid model induces net momentum in Fig. 2(a). With the inclusion of compressibility in Fig. 2(b), no net momentum is driven, and the magnitude of the flow is reduced by 2 orders of magnitude. This breakdown in momentum conservation results from using rf fields based on a compressible plasma response in a flow model that is incompressible.

In the kinetic result of Fig. 2(c), the rf pressure is about a factor of 5 less than the Reynolds stress and is exactly canceled by the EM force giving no net poloidal flow. Physically, since $k_y = 0$ (i.e., no net perpendicular momentum input), perpendicular momentum transport is required to induce poloidal flow. However, both LD and TTMP are $l = 0$ resonances ($\omega \approx k_z v_{\mathrm{th}}$) and transfer energy and parallel momentum directly to electrons with little perpendicular motion. Thus, perpendicular interactions apparently require ion-cyclotron resonances ($l \geq 1$) with scale lengths comparable to the ion Larmor radius. Even if k_y were finite, the momentum density of the wave is too small to drive significant flow in the y direction.

The last result, in Fig. 3, is closest to IBW experiments that employ resonant ion absorption. In this case, the magnetic field is reduced to 3.26 T, which puts the third harmonic resonance behind the antenna and gives very strong absorption at the second harmonic of D in front of the antenna. The compressible calculation in Fig. 3(b) shows a significant flow feature in front of the second harmonic resonance even though its magnitude is reduced by about a factor of 30 when compared with the incompressible analysis. The kinetic pressure model gives a still smaller flow, and the second, negative-going feature is absent. Overall, momentum conservation is preserved since the narrow positive-going peak sits on a much smaller and wider negative feature.

To evaluate the possibilities for turbulence suppression in Figs. 1–3, the approximate flow shear can be calculated by differentiating the poloidal flow velocity with respect to R. The magnitude of the shear needed for turbulence suppression has been estimated in Ref. [1] and is approximately $2 \times 10^5\ \mathrm{s}^{-1}$ for Alcator C-Mod parameters. For the case in Fig. 1, the power level of 1 MW produces flow shear in the required range. In Fig. 3(c), the flow shear for 1 MW is approximately 10 times larger than required.

Present IBW flow drive experiments have frequencies that are at high harmonics of the ion-cyclotron frequency, typically 5 times $\Omega_{c,i}$ [6,7]. Results presented in this paper cannot be directly compared with these experiments

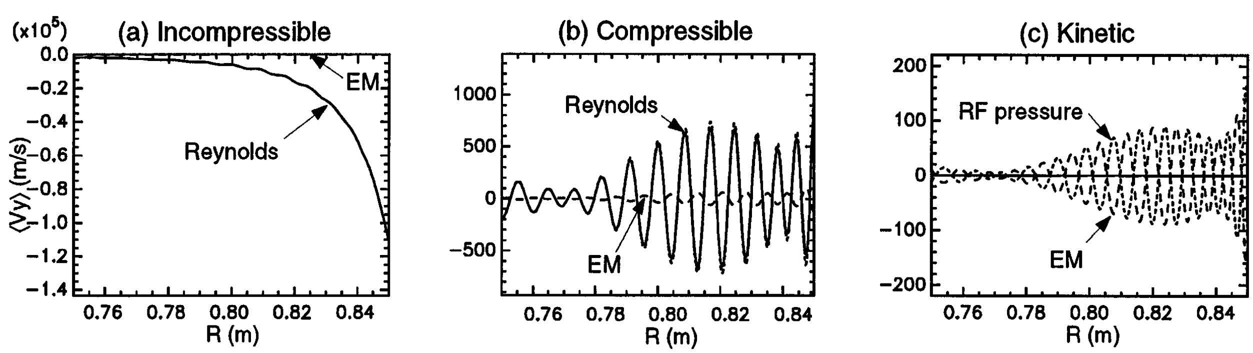

FIG. 2. Poloidal flow velocity for directly launched IBW absorbed by electron LD and TTMP with 2% He^3 in D, $f = 44$ MHz, $B(0) = 4.0$ T, and $k_z = 10\ \mathrm{m}^{-1}$: (a) incompressible fluid, (b) compressible fluid, and (c) kinetic model.

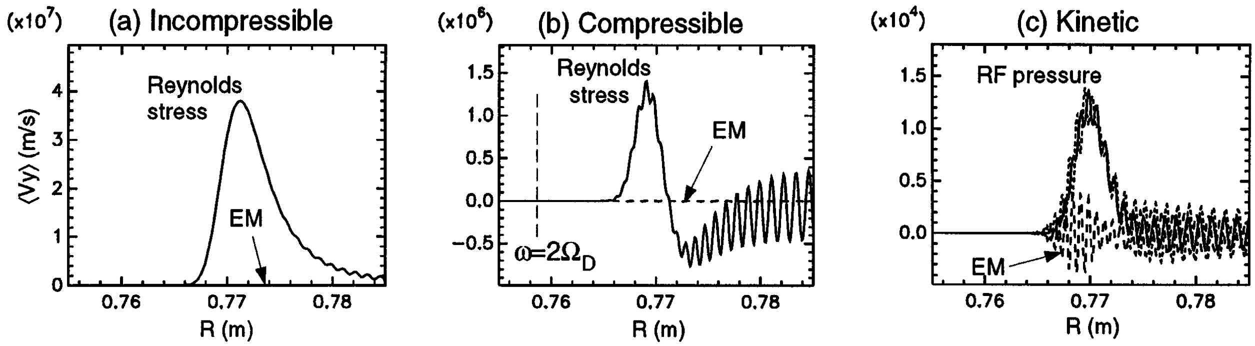

FIG. 3. Poloidal flow velocity for directly launched IBW absorbed by second harmonic ion-cyclotron damping in a D plasma with $f = 44$ MHz, $B(0) = 3.26$ T, and $k_z = 10\ \mathrm{m}^{-1}$: (a) incompressible fluid, (b) compressible fluid, and (c) kinetic model.

because the third-order gyroradius expansion can describe only ion interactions at frequencies near or below the third harmonic. But if the results in Fig. 3 are roughly applicable to higher harmonics, a several-fold reduction in predicted flow shear might be expected as a result of including compressibility or use of the kinetic rf pressure. Even with this reduction, the correspondence between experiment and model might still be reasonable. The needed level of flow shear is uncertain, and it may not be necessary for rf to provide all of the drive. Some fraction of the flow could be driven by Reynolds stress resulting from the plasma turbulence itself. In addition, the experimental flow measurements are difficult, and several possibly significant effects are excluded from the present models. These include the radial transport needed to maintain ambipolarity in the presence of rf forces, finite k_y, finite density and magnetic field gradients, and two-dimensional (2D) effects accounting for both spatial variation in the resonant interaction region and damping of 2D flow structures. Also, the scale length of the flow structure in the present models is small (on the order of an ion Larmor radius), and this regime has not been evaluated for flow stabilization. Any of these effects could reduce or increase model estimates for rf-driven flows and/or critical values for turbulence suppression.

We conclude that both compressibility and second-order kinetic rf pressures can have a significant effect on rf-driven flows. Compressibility is particularly important for longitudinal waves such as IBW. For all cases, the flows predicted by the kinetic pressure model are significantly different from those indicated by the Reynolds-stress-based analysis because of finite Larmor radius effects and/or the sensitivity of the net flow to a near cancellation of the EM and rf pressure forces.

With respect to flow drive prospects, the present model indicates that for $k_y = 0$, significant flows cannot be driven by electron LD and TTMP alone. But ion-cyclotron damping of either fast waves or IBW remains a promising technique for driving the sheared flow needed for reduced plasma turbulence and improved plasma confinement. Given the range of potentially important physics issues not included in the present models (for example, higher harmonic interactions), more experiments are needed to point toward the essential physics.

The authors thank K. H. Burrell, P. H. Diamond, M. Murakami, J. R. Myra, and colleagues at Oak Ridge National Laboratory for helpful discussions. Research was sponsored by the Office of Fusion Energy Sciences, U.S. Department of Energy, under Contract No. DE-AC05-96OR22464 with Lockheed Martin Energy Research Corp.

[1] H. Biglari, P. H. Diamond, and P. W. Terry, Phys. Fluids B **2**, 1 (1990).
[2] G. G. Craddock and P. H. Diamond, Phys. Rev. Lett. **67**, 1535 (1991).
[3] G. G. Craddock, P. H. Diamond, M. Ono, and H. Biglari, Phys. Plasmas **1**, 1944 (1994).
[4] F. Y. Gang, Phys. Fluids B **5**, 3835 (1993).
[5] C.-Y. Wang, E. F. Jaeger, D. B. Batchelor, and K. L. Sidikman, Phys. Plasmas **1**, 3890 (1994).
[6] T. Seki *et al.*, Nucl. Fusion **32**, 2189 (1992).
[7] B. LeBlanc *et al.*, Phys. Plasmas **2**, 741 (1995).
[8] T. H. Stix, in *Waves in Plasmas* (American Institute of Physics, New York, 1992).
[9] R. R. Mett, Phys. Fluids B **4**, 225 (1991).
[10] J. R. Cary and A. N. Kaufman, Phys. Fluids **24**, 1238 (1981).
[11] E. F. Jaeger, D. B. Batchelor, and H. Weitzner, Nucl. Fusion **28**, 53 (1988).
[12] P. T. Bonoli *et al.*, Phys. Plasmas **4**, 1774 (1997).